Anesthesiology 2007; 107:117–27

Contribution of Calcium Channel Subtypes to the Intracellular Calcium Signal in Sensory Neurons

The Effect of Injury

Andreas Fuchs, M.D.,* Marcel Rigaud, M.D.,† Constantine D. Sarantopoulos, M.D., Ph.D.,‡ Patrick Filip, M.D.,§ Quinn H. Hogan, M.D.‖

Background: **Although the activation-induced intracellular Ca^{2+} signal is disrupted by sensory neuron injury, the contribution of specific Ca^{2+} channel subtypes is unknown.**

Methods: **Transients in dissociated rat dorsal root ganglion neurons were recorded using fura-2 microfluorometry. Neurons from control rats and from neuropathic animals after spinal nerve ligation were activated either by elevated bath K^+ or by field stimulation. Transients were compared before and after application of selective blockers of voltage-activated Ca^{2+} channel subtypes.**

Results: **Transient amplitude and area were decreased by blockade of the L-type channel, particularly during sustained K^+ stimulation. Significant contributions to the Ca^{2+} transient are attributable to the N-, P/Q-, and R-type channels, especially in small neurons. Results for T-type blockade varied widely between cells. After injury, transients lost sensitivity to N-type and R-type blockers in axotomized small neurons, whereas adjacent small neurons showed decreased responses to blockers of R-type channels. Axotomized large neurons were less sensitive to blockade of N- and P/Q-type channels. After injury, neurons adjacent to axotomy show decreased sensitivity of K^+-induced transients to L-type blockade but increased sensitivity during field stimulation.**

Conclusions: **All high-voltage–activated Ca^{2+} current subtypes contribute to Ca^{2+} transients in sensory neurons, although the L-type channel contributes predominantly during prolonged activation. Injury shifts the relative contribution of various Ca^{2+} channel subtypes to the intracellular Ca^{2+} transient induced by neuronal activation. Because this effect is cell-size specific, selective therapies might potentially be devised to differentially alter excitability of nociceptive and low-threshold sensory neurons.**

THE pattern of rise and fall of intracellular Ca^{2+} levels ($[Ca^{2+}]_c$) initiated by depolarization-induced Ca^{2+} influx (I_{Ca}) is regulated by complex interactions of plasmalemmal Ca^{2+} influx, intracellular buffering, uptake, release from intracellular stores, and extrusion mechanisms.[1] The resulting Ca^{2+} transient regulates neuronal function, including cell development, excitability, neurotransmitter release, genetic expression, and apoptotic cell death.[2] Because the rise in $[Ca^{2+}]_c$ induced by neuronal activity lasts seconds compared with the few-millisecond duration of individual action potentials, the Ca^{2+} transient provides a time-integrated signal encoding neuronal activity history.[3] Through these mechanisms, altered Ca^{2+} dynamics play a central role in pathologic processes in neurologic disease.

Critical changes in the intracellular Ca^{2+} signal of primary sensory neurons contribute to hyperalgesia after peripheral nerve injury. Specifically, influx of Ca^{2+} through high- and low-voltage–activated Ca^{2+} channels is reduced after chronic constriction of the sciatic nerve[4] or ligation of the fifth lumbar (L5) spinal nerve.[5] Further, resting $[Ca^{2+}]_c$ is decreased[6] and the activity-induced Ca^{2+} transient is disrupted[7] after experimental peripheral nerve injury accompanied by hyperalgesic behavior in rats. Primary sensory neurons of the dorsal root ganglia (DRGs) express a variety of voltage-gated Ca^{2+} channel subtypes that can be distinguished according to their pharmacologic and electrophysiologic properties.[8–10] The various channels that conduct L, N, P/Q, R, and T subtypes of I_{Ca} are variably expressed in DRG neurons of different sizes.[11,12] In addition, the subtypes are functionally diverse and linked to specific Ca^{2+} regulated processes, partly on the basis of subcellular colocalization.[13] We expect that the different subtypes likewise do not contribute equally to the generation of the activity-induced intracellular Ca^{2+} transient, although this has not been examined in sensory neurons. Further, developing treatments for neuropathic pain would be aided by understanding how injury affects individual Ca^{2+} channel subtypes in generating the Ca^{2+} signal.

We therefore examined the sensitivity to subtype-specific Ca^{2+} channel blockers of activity-induced Ca^{2+} transients. Using digital microfluorometry, dissociated DRG neurons from control animals were compared with neurons from animals demonstrating hyperalgesic behavior after peripheral nerve trauma by spinal nerve ligation (SNL). This model allows separate study of L5 DRG neurons that are injured by axotomy *versus* L4 neurons exposed to inflammatory mediators induced by wallerian degeneration of adjacent L5 fibers in the shared sciatic nerve.[14,15]

* Research Fellow, Department of Anesthesiology, Medical College of Wisconsin. Staff Anesthesiologist, Department of Anesthesiology and Intensive Care Medicine, Medical University of Graz, Graz, Austria. † Research Fellow, Department of Anesthesiology, Medical College of Wisconsin. Resident, Department of Anesthesiology and Intensive Care Medicine, Medical University of Graz, Graz, Austria. ‡ Associate Professor, § Resident, Department of Anesthesiology, Medical College of Wisconsin. ‖ Professor, Department of Anesthesiology, Medical College of Wisconsin. Anesthesiologist, Milwaukee Veterans Administration Hospital, Milwaukee, Wisconsin.

Received from the Department of Anesthesiology, Medical College of Wisconsin, Milwaukee, Wisconsin. Submitted for publication January 25, 2006. Accepted for publication January 26, 2007. Supported in part by grant No. NS-42150 from the National Institutes of Health, Bethesda, Maryland.

Address correspondence to Dr. Hogan: Department of Anesthesiology, Medical College of Wisconsin, Room M4280, 8701 Watertown Plank Road, Milwaukee, Wisconsin 53226. qhogan@mcw.edu.

Materials and Methods

All procedures were approved by the animal care and use committee of the Medical College of Wisconsin, Milwaukee, Wisconsin.

Injury Model

Male adult Sprague-Dawley rats (Charles River Laboratories Inc., Wilmington, MA) weighing 160–180 g were randomly assigned to an SNL group or a control group. SNL was performed similar to the originally reported technique.[16] During anesthesia with isoflurane (2–3%) in oxygen, the right lumbar paravertebral region was exposed. After subperiosteal removal of the sixth lumbar transverse process, both the right L5 and L6 spinal nerves were tightly ligated with 5-0 silk suture and transected distal to the ligature. No muscle was removed, the intertransverse fascia were incised only at the site of the two ligations, and articular processes were not removed. The lumbar fascia was closed by 4-0 resorbable polyglactin suture, and the skin was closed with staples. In control rats, only lumbar skin incision and closure was performed. After surgery, the rats were returned to the colony, where they were kept in individual cages under normal housing conditions.

Sensory Testing

Identification of hyperalgesia was performed as described previously, using a method that has high specificity for heightened sensory responsiveness after nerve injury.[17] Briefly, at least 1 day after arrival in the animal care facility, rats were brought to the testing area for 4 h of familiarization with handling and the environment. Hind paws were stimulated in random order with a 22-gauge spinal needle applied with pressure adequate to indent but not penetrate the plantar skin 2 days before surgery and on 3 separate postoperative days. Control rats showed only a brief withdrawal. SNL animals that displayed a hyperalgesia-type response with sustained lifting, licking, chewing, or shaking of the paw were considered to express neuropathic pain behavior. This distinguished nerve injury–related behavior more selectively than withdrawal from von Frey stimulation.

Cell Isolation and Plating

The L4 and L5 DRGs were removed from control rats and hyperalgesic SNL rats (studied separately) after isoflurane anesthesia and decapitation. The operative field was perfused with cold, oxygenated, Ca^{2+} and magnesium chloride–free Hanks Balanced Salt Solution. Minced ganglia were enzymatically dissociated in a solution containing 0.018% liberase blendzyme 2 (Roche Diagnostics Corp., Indianapolis, IN), 0.05% trypsin (Sigma, St. Louis, MO), and 0.01% deoxyribonuclease 1 (150,000 U; Sigma) in 4.5 ml DMEM F12 (Gibco, Invitrogen Corp., Carlsbad, CA) for 60 min at 37°C. Cells were harvested by centrifugation and resuspended in a culture medium consisting of 0.5 mM glutamine, 0.02 mg/ml gentamicin, 100 ng/ml nerve growth factor 7S (Alomone Labs, Jerusalem, Israel), 2% (vol/vol) B-27 supplement (Life Technologies, Rockville, MD), and 98% (vol/vol) neurobasal medium A 1X (Life Technologies) for plating onto poly-L-lysine–coated 12-mm glass coverslips (Deutsche Spiegelglas; Carolina Biologic Supply, Burlington, NC), plating from two to four slips per ganglion. Cells were incubated for 2–3 h in humidified incubator at 37°C with 95% air and 5% CO_2 before dye loading, and were studied within 5 h of dissociation.

Calcium Microfluorometry

Cytoplasmic Ca^{2+} Measurement. Cells were loaded with the ratiometric Ca^{2+} indicator fura-2 AM (2.5 μm in 0.1% Pluronic F-127; Molecular Probes, Eugene, OR) for 45 min at room temperature and then washed three times with a Tyrode solution consisting of 140 mM NaCl, 4 mM KCl, 2 mM $CaCl_2$, 2 mM $MgCl_2$, 10 mM glucose, and 10 mM HEPES. Cells were left in a dark environment for 30 min for dye de-esterification. Coverslips were mounted in a 500-μl recording chamber superfused with room temperature (22°C) Tyrode solution at a gravity driven flow rate of 2 ml/min, and imaged at 400× magnification using an inverted microscope (Nikon Diaphot 200; Nikon, Tokyo, Japan) and cooled charge-coupled device camera (Cool Snap; fx-Photometrics, Tucson, AZ). Cell diameter was determined by calibrated video image. On bright-field examination, neurons were excluded from measurement if they showed evidence of lysis or crenulation of their surface, because these cells showed unstable recordings, and also if they had overlying glial satellite cells. Only one field was studied per slip. Autofluorescence of unloaded cells had a signal strength of less than 5% of the fluorescence of loaded cells. Emitted fura-2 fluorescence was recorded at 510 ± 20 nm wavelength during alternating 340- and 380-nm excitation (DG-4; Sutter, Novato, CA). The ratio (R) of fluorescence excited by 340 nm divided by fluorescence excited by 380 nm was determined on a pixel-by-pixel basis. The frame capture period was 200 ms at intervals of 1–20 s. Each neuron was specified as a region of interest in the digital image (MetaFluor; Universal Imaging Corporation, Downingtown, PA) for separate averaging of R of the region, and an additional background area was recorded in each field for on-line subtraction of background fluorescence. R is directly related to $[Ca^{2+}]_c$.[18] Because this study examines ratio changes, we report R (in ratio units [R.u.]) and do not convert R into actual $[Ca^{2+}]_c$.

Neuronal Stimulation. In most of the experiments, the first Ca^{2+} transient was elicited by a 5-s bath application of Tyrode solution containing elevated K^+ concentration (50 mm) with reciprocal decrease in Na^+ concentration, through a microperfusion system (onset

time less than 200 ms) 125 μm upstream from the imaged field. A four-valve gravity-driven microperfusion system (BPS-4; ALA, Westbury, NY) was digitally controlled by Clampex8.1 software (Axon Instruments, Foster City, CA). After recovery of the transient to a stable baseline level, a subtype blocker was applied for 4 min followed by a second 5-s K^+ depolarization. Only one recording was performed per slip. This depolarization technique maximally activates Ca^{2+} handling processes by producing a sustained depolarization that is considerably longer than a short train of action potentials, although it could duplicate the Ca^{2+} load provided by a sustained burst of intense pathologic activity. In other experiments, neurons were excited by field stimulation rather than high K^+, to trigger natural action potentials.[19] Constant voltage stimuli (1-ms biphasic pulses, 10 Hz for 3 s; SIU-102; Warner Instruments, Hamden, CT) were passed between two platinum electrodes positioned on either side of the target neurons (RC-21BRFS chamber; Warner Instruments). Voltage amplitude was monitored to maintain consistent stimulation at ±30 V throughout each protocol.

Electrophysiologic Recording

In a small subset of neurons, we examined membrane potential and inward I_{Ca} through channel subtypes to identify the extent of depolarization, confirm the activation of the various Ca^{2+} channel subtypes, and assure the adequacy of our blocking agents. Recordings were made from dissociated neurons in both current clamp and voltage clamp mode using standard patch clamp techniques.[4] Briefly, pipettes with resistance of 2–3 MΩ were filled with solution containing 120 mM KCl, 5 mM Na-ATP, 0.4 mM Na-GTP, 5 mM EGTA, 2.25 mM $CaCl_2$, 5 mM $MgCl_2$, and 20 mM HEPES. It was buffered to a pH of 7.4 with KOH and had an osmolarity of 295–300 mOsm/l adjusted with sucrose when necessary. During current clamp recording, the cells were bathed in the same Tyrode solution as used for $[Ca^{2+}]_c$ recording, whereas voltage clamp recordings were performed with an external solution of the following composition: 160 mM tetraethylammonium chloride (TEA-Cl), 2 mM $CaCl_2$, 10 mM HEPES, 1 mM 4-aminopyridine, and 0.001 mM tetrodotoxin, at a pH of 7.4 with TEA-OH and an osmolarity of 300 mOsm/l, adjusted with sucrose when necessary. Currents sensitive to specific blockers were calculated as the difference between the current measured immediately before and after the application of that drug, as a fraction of the total baseline current.

Agents

Each Ca^{2+} channel subtype blocker was applied at the lowest effective concentration to achieve optimal selectivity, based on previous reports[20–26] and on our patch clamp studies in DRG neurons (data not shown). Specifically, we blocked L-type channels with 10 μM nicardipine (IC_{50} 4.4 μM[27]), N-type channels with 200 nM SNX-111 (IC50 6 nM,[23] and 30 nM by our patch clamp experiments), 200 nM P/Q-type channels with ω-agatoxin-IVA (Aga-IVA; IC_{50} 3 nM for P-type, 120 nM for Q-type,[26] and approximately 50 nM for undifferentiated P/Q-type channels by our patch clamp experiments), and R-type channels with 100 nM SNX-482 (IC_{50} 30 nM,[21] and approximately 30 nM by our patch clamp experiments). The concentration chosen for mibefradil (200 nM) was based on previous research[22] showing blockade of 70% of isolated T-type current. In addition, the L-type channel agonist Bay K 8644 (2 μM) was used to test the effects of elevating neuronal Ca^{2+} entry.[28] SNX-111 was the kind gift of Scott Bowersox, Ph.D. (Neurex Corporation, Menlo Park, CA), whereas SNX-482 and Aga-IVA were purchased from Peptides International (Louisville, KY). All other agents were purchased from Sigma-Aldrich Co. (St. Louis, MO). All drugs were prepared daily using aliquots from frozen stock solutions to obtain the working concentrations dissolved in Tyrode solution, except nicardipine, which also contained 0.1% polyethylene glycol. Application of agents was initiated 3 min before recording, with the exception of SNX-111 and SNX-482, which are fast acting and were applied for 30 s before recording. Applications were continued during stimulation and transient response.

Analysis and Statistics

Dimensions of the Ca^{2+} transient induced by stimulation were determined by digital trace analysis (Axograph 4.7; Axon Instruments), as detailed in figure 1. Specifically, transient amplitude was determined from the previous resting level, and the duration determined as the time for $[Ca^{2+}]_c$ to achieve 80% recovery to the resting level. Because a change in transient amplitude secondarily alters the 80% level at which duration is determined, a decrease in amplitude artifactually prolongs the apparent duration of the transient when measured this way. We therefore in addition calculated the area under the curve by digital analysis. We have previously observed a predictable shift in the resting level after a transient,[7] so this was also measured. Although these features of the transient are regulated by various Ca^{2+} uptake, release, and expulsion processes in the neuron (see discussion in Fuchs *et al.*[7]), their specific functional significance is incompletely understood.

Neurons were divided into two groups with diameters above or below 34 μm[6,29] to partially segregate the overlapping nociceptive and nonnociceptive neuron categories.[30] The number of cells tested is referred to as *n*. In all determinations, data are derived from at least seven animals. The effect of an agent on a measured parameter was examined by paired *t* test. Cell numbers were large, so parametric analysis by analysis of variance was used to determine main effects of injury. *Post hoc* comparisons between control, SNL L4, and SNL L5 groups were per-

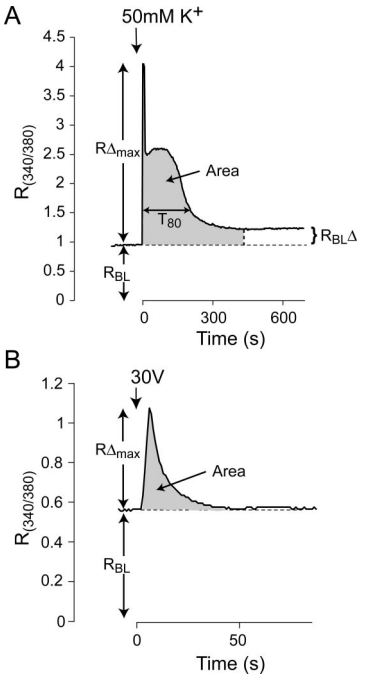

Fig. 1. Measures of the Ca^{2+} transient indicated by the fluorescence ratio ($R_{340/380}$). Typical trace after K^+ stimulation (*A*) shows baseline ratio (R_{BL}), transient amplitude above baseline ($R\Delta_{max}$), transient duration to 80% recovery (T_{80}), transient area (*shaded*), and the offset of the posttransient baseline above the original baseline ($R_{BL}\Delta$). Transients after field stimulation (*B*) typically lack a plateau. Because the measure of T_{80} is then highly sensitive to transient amplitude, this measure was not separately determined.

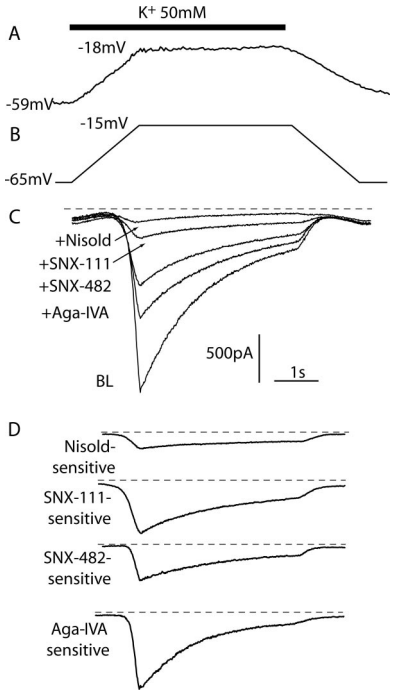

Fig. 2. Electrophysiology associated with neuron depolarization with application of 50 mM K^+. The transmembrane potential (*A*) was recorded during application of K^+, indicated by the *bar*. A similar voltage command protocol (*B*) was used during subsequent current recordings. Sequential current traces (*C*) were recorded during cumulative application of blockers, starting with baseline (BL), then ω-agatoxin-IVA (Aga-IVA, 200 nM), then addition of SNX-482 (200 nM), SNX-111 (200 nM), and nisoldipine (Nisold, 200 nM). Subtracted traces (*D*) show the current sensitive to Aga-IVA, SNX-482, SNX-111, and nisoldipine.

formed conservatively using the Bonferroni test (Statistica 6.0; StatSoft, Tulsa, OK). Similarly, the effects of different drugs on control neurons were compared by analysis of variance. Measures are reported as mean ± SEM. Differences were considered significant at $P < 0.05$.

Results

Behavioral Responses

Dorsal root ganglia were removed 25 ± 1 days after injury in rats with hyperalgesia after SNL (n = 30). In these rats, hyperalgesia-type responses occurred in 42 ± 4% of needle applications. Examination during harvest confirmed accurate placement of ligatures and section for all SNL animals. Control rats (n = 34) did not develop hyperalgesic behavior (1 ± 1% hyperalgesic response rate; $P < 0.001$ *vs.* SNL), and DRGs were removed 23 ± 1 day after skin incision surgery.

Electrophysiologic Validation of High K^+ Stimulation

Because the threshold for activation of voltage-gated Ca^{2+} channel subtypes ranges from −70 to −20 mV,[31] we first examined the effect of the 50 mM K^+ depolarization protocol on neuronal transmembrane voltage. Potassium application depolarized the transmembrane potential to −13 ± 0.9 mV (n = 5; fig. 2A), which was sustained during the application. This confirms that our protocol is adequate to activate all channel subtypes. Although high K^+ depolarization is commonly performed for neuronal activation, contributions by Ca^{2+} channel subtypes triggered by this method have not been examined. We therefore recorded I_{Ca} by patch clamp technique in a group of medium-sized neurons (diameter 32 ± 4 μm, n = 8) using a voltage command protocol that duplicated the voltage recorded during K^+ depolarization (fig. 2B). The overall I_{Ca} showed progressive inactivation but included a sustained component that persisted for the full 5 s of depolarization (fig. 2C), which supports our previous finding that cellular Ca^{2+} load increases with greater duration of depolarization.[6]

We identified currents carried by individual Ca^{2+} channel subtypes by sequential application of selective blockers and determined the components sensitive to these blockers by calculating difference currents (fig. 2D). The L-type blocker nisoldipine (200 nM, based on an IC_{50} of 40 nM from our patch clamp studies; data not shown) eliminated 46 ± 11% of the peak current, the N-type toxin SNX-111 blocked 35 ± 7%, P/Q blockade with Aga-IVA eliminated 9 ± 6%, and the R-type toxin SNX-482 blocked 10 ± 5% of peak current. (Because of large

Table 1. Measures of Transient Induced by Potassium Depolarization in Neurons Categorized by Size

	Small Neurons				Large Neurons			
	Main Effect *P*	Control (289)	SNL L4 (137)	SNL L5 (188)	Main Effect *P*	Control (72)	SNL L4 (41)	SNL L5 (41)
R_{BL}, R.u.	< 0.001	0.68 ± 0.01	0.73 ± 0.01**	0.53 ± 0.01**†	< 0.001	0.75 ± 0.02	0.71 ± 0.02	0.59 ± 0.02**††
$R\Delta_{max}$, R.u.	0.35	2.27 ± 0.06	2.33 ± 0.09	2.42 ± 0.09	< 0.001	1.01 ± 0.10	1.50 ± 0.24	2.14 ± 0.21**†
T_{80}, min	< 0.001	1.71 ± 0.07	1.81 ± 0.10	0.61 ± 0.04**††	0.045	1.38 ± 0.19	1.28 ± 0.16	0.77 ± 0.10*
Area, R.u. · min	< 0.001	1.87 ± 0.08	1.91 ± 0.12	0.84 ± 0.04**††	0.3	0.70 ± 0.08	0.94 ± 0.18	0.79 ± 0.11
$R_{BL}\Delta$, R.u.	< 0.001	0.15 ± 0.01	0.17 ± 0.01*	0.05 ± 0.00**††	0.006	0.08 ± 0.01	0.08 ± 0.01	0.05 ± 0.01**†

Number in parentheses indicates n for neurons. Values are expressed as mean ± SE. Main effect indicates *P* for overall analysis of variance.

Individual comparisons between groups are as follows: different from control: * $P < 0.05$, ** $P < 0.01$; different from SNL L4: † $P < 0.05$, †† $P < 0.01$.

Area = area under the transient until stable baseline is reached; $R_{BL}\Delta$ = shift in baseline; $R\Delta_{max}$ = transient amplitude; R.u. = ratio units of fluorescence at 340 nm excitation/fluorescence at 380 nm excitation; SNL L4 = fourth lumbar ganglion after spinal nerve ligation; SNL L5 = fifth lumbar ganglion after spinal nerve ligation; T_{80} = duration of transient to 80% recovery.

interneuronal variability, the example shown in fig. 2 does not duplicate these average values.) Therefore, the full spectrum of high-voltage–activated Ca^{2+} current subtypes are triggered by our high K^+ stimulation protocol. Interestingly, all types showed a current component sustained even out to 5 s with type of voltage command. This is consistent with a previous report in which sustained currents in small rat DRG neurons included components that were sensitive to nitrendipine (L-type current) and ω-conotoxin GVIA (N-type), as well as a residual resistant component.[25]

K^+-induced Transients in Control Neurons

Similar to our previous findings,[6] 5-s depolarization by elevated K^+ produced prolonged Ca^{2+} transients (table 1 and fig. 1), with a sustained plateau during the transient resolution in most cases (93% for small neurons, 57% for large neurons). After the transient, $[Ca^{2+}]_c$ did not return to the previous baseline but rather settled to a sustained elevated baseline.

Effect of I_{Ca} Blockers on K^+-induced Transients in Control Neurons

We have previously demonstrated that the Ca^{2+} transient induced by neuronal depolarization is dependent on Ca^{2+} entry through voltage-gated Ca^{2+} channels. Specifically, we achieved complete blockade by withdrawal of bath Ca^{2+} or application of the nonspecific blocker cadmium.[6] To confirm that the specific subtype blockers used in the current study account for all the sources of voltage-gated Ca^{2+} entry during neuronal stimulation, we measured Ca^{2+} transients before and after simultaneous application of all subtype blockers (fig. 3). This eliminated 95 ± 2% of transient amplitude (n = 12 small neurons; $P < 0.001$), shortened the transient duration by 94 ± 2% ($P < 0.001$), and nearly eliminated the area of the transient (decreased by 99 ± 1%; $P < 0.001$). These findings also confirm that the subtype blockers had a sustained effect although they were not present in the solutions during 5-s depolarization or during the resolution of the transient, and that the concentrations and duration of application were adequate to achieve blockade. There was no direct effect of the blockers on resting $[Ca^{2+}]_c$ when applied together nor when given individually (data not shown).

Application of vehicle solution containing Tyrode solution and cytochrome *c* had no effect on the Ca^{2+} transient (n = 14). The effect of individually applied voltage-gated Ca^{2+} channel subtype blockers (table 2 and fig. 4) was to inhibit the transient and limit the baseline offset after the transient. Block of L-type channels with nicardipine decreased the transient amplitude and area and decreased the baseline offset, in both large and small neurons. Nicardipine was delivered in a vehicle containing 0.1% polyethylene glycol, which alone diminished the baseline offset (change of −0.09 ± 0.02 R.u., n = 14; $P < 0.001$). We therefore performed further experiments with the L-type blocker nitrendipine (10 μM) in a Tyrode solution that did not require polyethylene glycol. This agent produced comparable changes as nicardipine, including an identical loss of baseline offset (change of −0.11 ± 0.02 R.u., n = 15; $P < 0.001$).

Block of N-type channels with SNX-111, P/Q-type channels with Aga-IVA, and R-type channels with SNX-482 produced similar results. In all cases, transient amplitude and baseline offset were diminished in large and small neurons. Transient amplitude and area were de-

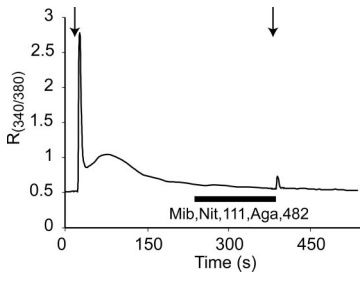

Fig. 3. Complete blockade of Ca^{2+} transient by combined administration of selective I_{Ca} subtype blockers. Application of T-type blocker mibefradil (Mib, 200 nM), L-type blocker nitrendipine (Nit, 10 μM), N-type blocker SNX-111 (200 nM), P/Q-type blocker ω-agatoxin-IVA (Aga-IVA, 200 nM), and R-type blocker SNX-482 (100 nM) eliminated the response to K^+ depolarization (50 mM for 5 s; *arrows*).

Table 2. Effects of Selective Ca^{2+} Channel Blockers on Potassium-induced Transients in Neurons Categorized by Size and Injury

		n (Neurons)			$R\Delta_{max}$, Change		
Agent	Size	Control	SNL L4	SNL L5	Control	SNL L4	SNL L5
Mibefradil (200 nM)	Lg	7	7	7	−19 ± 11	−7 ± 2*	−5 ± 9
	Sm	48	24	33	−10 ± 3**	−12 ± 2**	−11 ± 4**
Nicardipine (10 μM)	Lg	11	6	8	−55 ± 11**	−35 ± 7*	−21 ± 6
	Sm	57	25	29	−32 ± 2**	−18 ± 5**; C	−22 ± 5**
SNX-111 (200 nM)	Lg	37	12	11	−32 ± 4**	−34 ± 6*	−17 ± 10
	Sm	107	36	68	−20 ± 2**	−20 ± 3**	−10 ± 2**; C, L4
Aga-IVA (200 nM)	Lg	11	6	8	−20 ± 4**	−27 ± 7	−11 ± 6
	Sm	32	26	35	−8 ± 2**	−12 ± 3**	−7 ± 3
SNX-482 (100 nM)	Lg	6	10	7	−22 ± 6**	−26 ± 8**	−8 ± 2*
	Sm	45	26	23	−16 ± 3**	−7 ± 2*; C	−4 ± 2; C

Values are expressed as mean ± SE.

Significant agent effects: * $P < 0.05$, ** $P < 0.01$; comparisons between injury groups: C indicates $P < 0.05$ *vs.* control group, L4 indicates $P < 0.05$ *vs.* SNL L4 group.

Area = area under the transient until stable baseline is reached; Lg = large; n = number of neurons; $R_{Bl}\Delta$ = shift in baseline; $R\Delta_{max}$ = transient amplitude; R.u. = ratio units of fluorescence at 340 nm excitation/fluorescence at 380 nm excitation; Sm = small; SNL L4 = fourth lumbar ganglion after spinal nerve ligation; SNL L5 = fifth lumbar ganglion after spinal nerve ligation; T_{80} = duration of transient to 80% recovery.

creased in small neurons, but these parameters were variably affected in large neurons.

With available T-type blockers, the goal of complete current elimination is unattainable without substantial nonspecific effects on other channels. In Purkinje cells, 200 nM mibefradil blocks 70% of T-type current elicited from a resting potential of −70 mV (characteristic of resting DRG neurons).[22] This concentration thus produces substantial blockade but avoids nonspecific effects typical of micromolar concentrations, such as block of HVA currents[32] (especially L-type[33]) or Na^+ currents.[33] To examine for nonspecific effects, we tested higher concentrations of mibefradil in small neurons and found decreased transient area of 54 ± 6% with 1 μM (n = 11) and 89 ± 2% with 3 μM (n = 13). Because T-type currents make a minimal contribution to I_{Ca} in small neurons,[11,34] these findings indicate actions of mibefradil on other Ca^{2+} channel subtypes at these concentrations.

In the current study, T-type block with mibefradil at 200 nM concentration had no effect on K^+-induced transient measures in large neurons (table 2). In small neurons, mibefradil decreased transient amplitude and baseline offset but to a lesser extent than other blockers. Whereas studies measuring T-type current directly have found a subgroup of neurons with particularly large T-type I_{Ca},[11,34] we could not identify a subgroup that showed Ca^{2+} transients with a high mibefradil sensitivity.

Comparison of the blockade of individual subtypes in small neurons showed that the transient amplitude was most dependent on L- and N-type channels (fig. 4). The contribution of the various subtypes to the transient area was comparable for all subtypes except T, the blockade of which did not have an effect. L- and N-type channels had the greatest contribution to the baseline offset. For large neurons, L- and N-type channels also made the greatest contribution to the amplitude, area, and baseline offset of the transient.

Effect of I_{Ca} Amplification on K^+-induced Transients in Control Neurons

Because blockade of Ca^{2+} influx through voltage-gated channels reduced measures of the Ca^{2+} transient, we speculated that enhanced Ca^{2+} should have the opposite effect. Accordingly, we applied the L-type Ca^{2+} channel agonist Bay K 8644 (2 μM) to control neurons (17 small and 1 large) to increase Ca^{2+} entry during activation. Consistent with our expectations, transient duration was increased by 81 ± 11% ($P < 0.001$), transient area was increased by 66 ± 8% ($P < 0.001$), and transient amplitude was increased by 4 ± 3% ($P < 0.05$). Baseline offset was diminished by 0.04 ± 0.01 ($P < 0.05$).

Transients in Injured Neurons

The initial (preagent) stimulation of neurons from animals subjected to SNL showed changes that confirm our previous findings (table 1).[6,7] Specifically, small and large axotomized neurons from L5 developed a depressed baseline $[Ca^{2+}]_c$, more rapid transient resolution, and loss of the baseline offset. Large neurons in addition showed a greater transient amplitude. After SNL, small neurons from L4 developed and elevated baseline and a greater baseline offset after transient resolution. In the current data set, we in addition calculated transient area, which was decreased by axotomy in small neurons.

Effect of I_{Ca} Blockers on K^+-induced Transients in Injured Neurons

Because we have previously determined that injury of peripheral sensory neurons decreases the Ca^{2+} transient,[7] we therefore examined whether this injury effect

Table 2. Continued

T_{80}, % Change			Area, % Change			$R_{BL}\Delta$, Change in R.u.		
Control	SNL L4	SNL L5	Control	SNL L4	SNL L5	Control	SNL L4	SNL L5
65 ± 64	228 ± 97	−6 ± 36	41 ± 63	107 ± 64	−3 ± 33	−0.03 ± 0.02	−0.01 ± 0.02	−0.02 ± 0.01
21 ± 14	5 ± 17	−23 ± 35**	3 ± 11*	−9 ± 9*	−18 ± 7**	−0.03 ± 0.01**	−0.03 ± 0.01*	−0.03 ± 0.01**
21 ± 48	−28 ± 18	−20 ± 17	−60 ± 19*	−53 ± 10*	−25 ± 18	−0.12 ± 0.03**	−0.09 ± 0.02	−0.05 ± 0.01**
−20 ± 8**	−7 ± 17*	−4 ± 9*	−38 ± 7**	−26 ± 12	−20 ± 10	−0.11 ± 0.01**	−0.15 ± 0.01**; C	−0.04 ± 0.01**; C, L4
−7 ± 13**	−43 ± 5**	36 ± 11*; L4	−41 ± 4**	−57 ± 7**	24 ± 15; C, L4	−0.04 ± 0.01**	−0.06 ± 0.01**	0 ± 0.01; C, L4
−44 ± 3**	−37 ± 6**	−7 ± 6*; C, L4	−48 ± 3**	−36 ± 6**	−6 ± 9**; C, L4	−0.09 ± 0.01**	−0.09 ± 0.01**	−0.02 ± 0**; C, L4
−9 ± 12	5 ± 26	11 ± 17	−36 ± 7**	−18 ± 12	5 ± 14; C	−0.03 ± 0.01**	−0.01 ± 0.02	0 ± 0
−20 ± 6**	−34 ± 7**	−14 ± 5**	−22 ± 6**	−31 ± 7**	−10 ± 5*; L4	−0.07 ± 0.01**	−0.07 ± 0.02**	−0.01 ± 0**; C, L4
−1 ± 22	−26 ± 13*	−11 ± 14	−30 ± 10	−37 ± 11*	−11 ± 12	−0.04 ± 0.01*	−0.04 ± 0.01**	−0.02 ± 0.02
−32 ± 8**	−20 ± 7*	−20 ± 4**	−37 ± 6**	−19 ± 5**	−16 ± 4**; C	−0.07 ± 0.01**	−0.02 ± 0.01*; C	−0.01 ± 0.01; C

is selectively attributable to changes in certain Ca^{2+} channel subtypes by comparing the effect of the selective blockers in axotomized, adjacent, and control neurons (table 2 and fig. 5). The greatest differences were seen in small neurons after axotomy (L5), particularly in the response to SNX-111 and SNX-482. Specifically, the reduction in transient amplitude by SNX-111 was halved by axotomy, and the reduction of transient area was nearly eliminated. SNX-482 actions were also decreased by axotomy, particularly its effect on transient amplitude. Because axotomy largely eliminated the baseline offset, all drugs show a limited response in these cells compared with control neurons. The adjacent neurons of L4 show a decreased effect of nicardipine and SNX-482 on transient amplitude and a decreased effect of SNX-482 on baseline offset, but an increased effect of nicardipine on baseline offset. Axotomy of large neurons eliminates the decrease in transient area caused by SNX-111 and Aga-IVA.

Effect of I_{Ca} Blockers on Field Stimulation–induced Ca^{2+} Transients

Stimulation with 5-s K^+ application results in channel opening that much exceeds the duration during action potential trains, although the Ca^{2+} load may resemble that which follows a sustained burst of neuronal activity in pathologic conditions. To model more physiologic conditions, we used field stimulation[7] to examine the effect of specific Ca^{2+} channel subtype blockers during generation of natural action potentials (fig. 6). Experiments with control neurons stimulated this way confirm the sensitivity of the transient to SNX-111, SNX-482, and

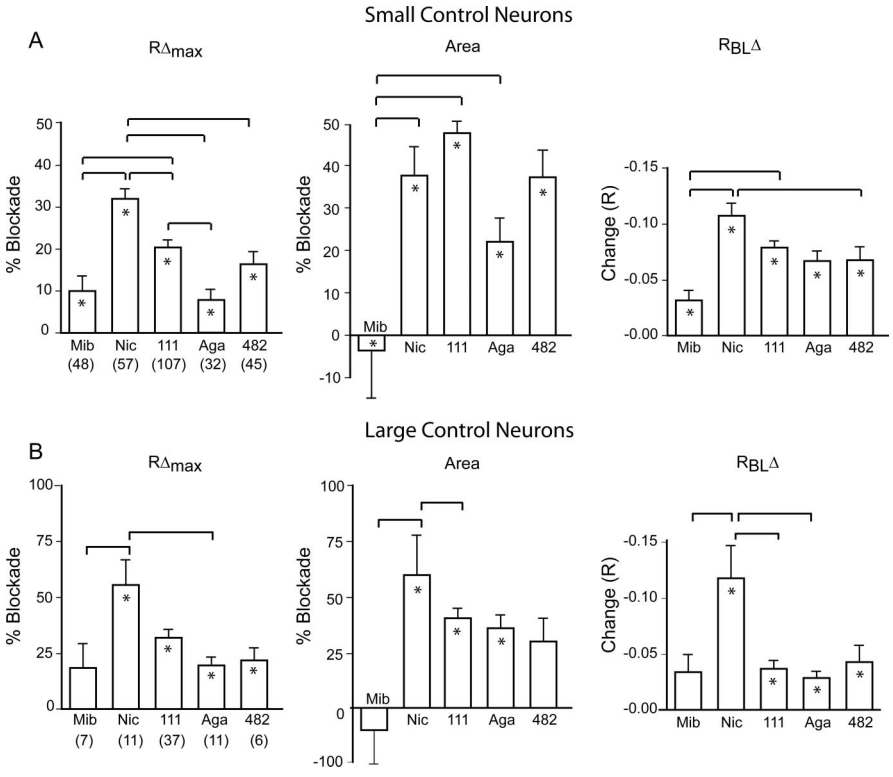

Fig. 4. Responses of Ca^{2+} transient measures to different Ca^{2+} channel subtype blockers in small (*A*) and large (*B*) control sensory neurons stimulated by high K^+. Mibefradil (Mib, 200 nM), nicardipine (Nic, 10 μM), SNX-111 ("111," 200 nM), ω-agatoxin-IVA (Aga, 200 nM), and SNX-482 ("482," 100 nM) were applied. Each neuron was exposed to only a single agent. An *asterisk* within the *bar* indicates a significant effect on the transient after application compared with baseline. There was a significant main effect between agents for each measure in each cell size category. *Brackets* indicate significant differences by *post hoc* paired comparisons (Bonferroni). Area = transient area; R = ratio of fluorescence excited by 340 nm divided by fluorescence excited by 380 nm; $R_{BL}\Delta$ = offset of the posttransient baseline above the original baseline; $R\Delta_{max}$ = transient amplitude. Numbers in parentheses (n) apply to each parameter for that neuronal size. Note that the scales are different in the positive and negative direction for Area in large neurons.

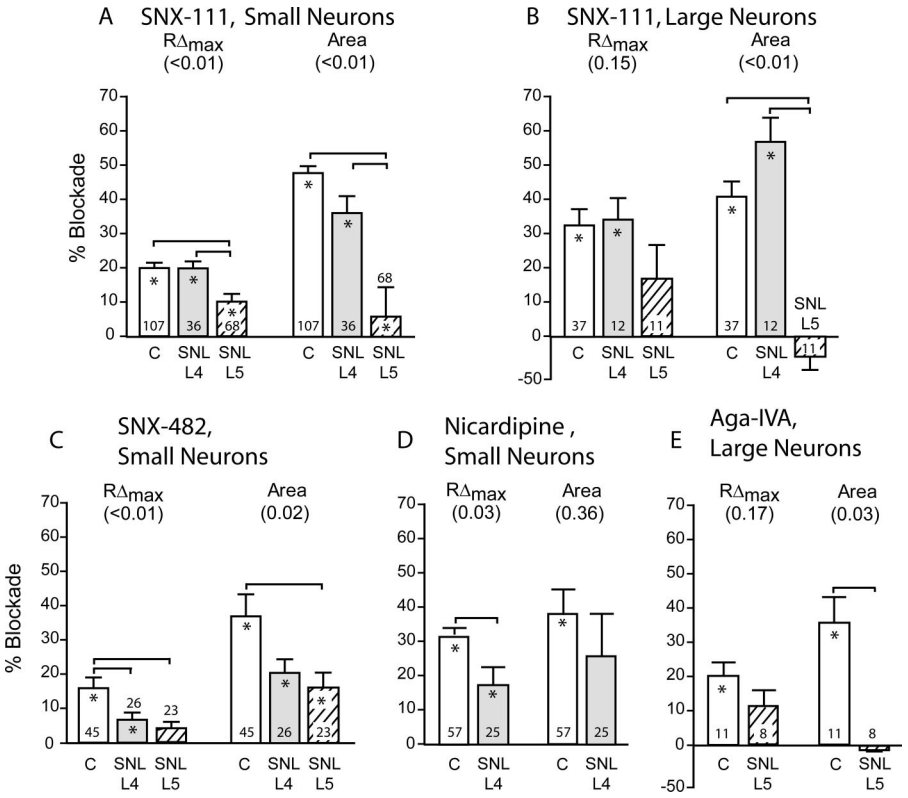

Fig. 5. Responses of K^+-stimulated Ca^{2+} transient measures to SNX-111 (200 nM) in small (*A*) and large (*B*) sensory neurons, to SNX-482 (100 nM) in small neurons (*C*), to nicardipine (10 μM) in small neurons (*D*), and to ω-agatoxin-IVA (200 nM) in large neurons (*E*). Blockers were applied to control neurons, and neurons dissociated from the fourth lumbar (L4) and L5 ganglion of rats after spinal nerve ligation (SNL). Each neuron was exposed to only a single agent. Results for neuronal groups without significant changes are not shown. An *asterisk* within the *bar* indicates a significant effect on the transient after application compared with baseline. Numbers in parentheses are main effect of injury using one-way analysis of variance or *t* test. *Brackets* indicate significant differences by *post hoc* paired comparisons. C = control; $R\Delta_{max}$ = transient amplitude. Numbers at the *base of the bars* are number of neurons per group.

Aga-IVA, although their actions on transient amplitude and area are generally greater than was observed with K^+ stimulation. Among these peptides, the greatest blockade during both types of stimulation was with SNX-111. We initially used nitrendipine (10 μM) for L-type channel blockade in these experiments, but we switched to nisoldipine (200 nM) when nitrendipine became unavailable. The results were comparable, and the pooled results are reported here. Whereas L-type blockade during K^+ stimulation had a large effect, minimal

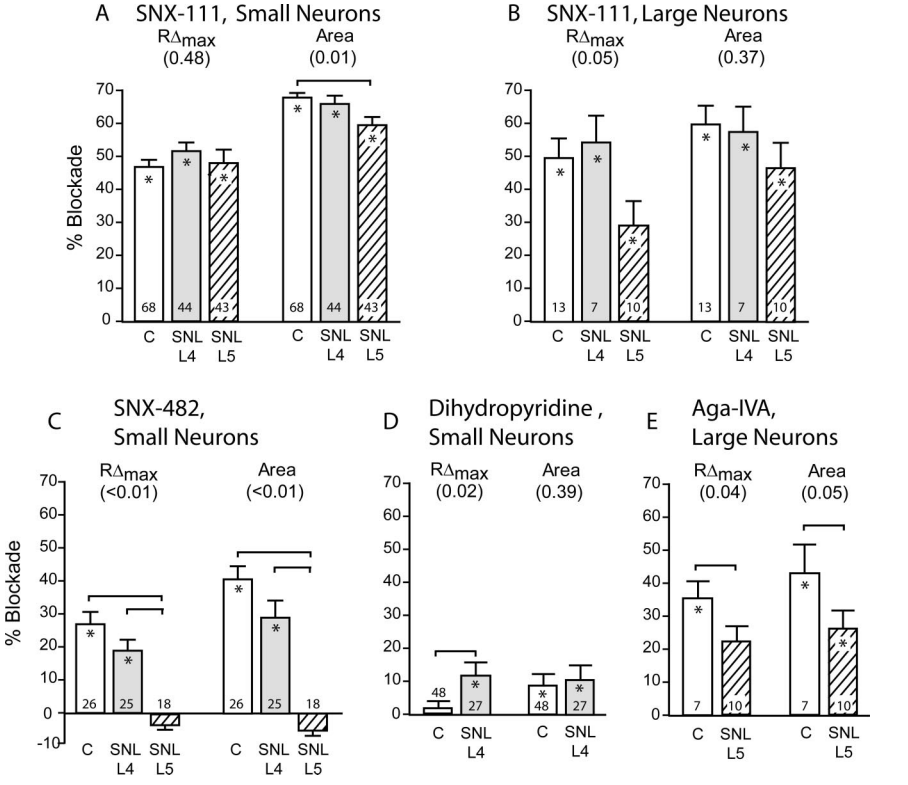

Fig. 6. Responses of field-stimulated Ca^{2+} transient measures to SNX-111 (200 nM) in small (*A*) and large (*B*) sensory neurons, to SNX-482 (100 nM) in small neurons (*C*), to nitrendipine (10 μM) or nisoldipine (200 nM) in small neurons (*D*; results did not differ and were combined), and to ω-agatoxin-IVA (200 nM) in large neurons (*E*). Agents were applied to control neurons and neurons dissociated from the fourth lumbar (L4) and L5 ganglion of rats after spinal nerve ligation (SNL). Each neuron was exposed to only a single agent. Results for neuronal groups without significant changes are not shown. An *asterisk* within the *bar* indicates a significant effect on the transient after application compared with baseline. Numbers in parentheses are main effect of injury using one-way analysis of variance or *t* test. *Brackets* indicate significant differences by *post hoc* paired comparisons. C = control; $R\Delta_{max}$ = transient amplitude. Numbers at the *base of the bars* are number of neurons per group.

sensitivity to L-type blockers was seen in transients triggered by field stimulation. This contrast is consistent with the noninactivating nature of L-type currents, which therefore will make a particularly large contribution to inward Ca^{2+} flux during the sustained depolarization caused by K^+ stimulation. In these experiments, we did not analyze the transient duration to 80% recovery, because field-stimulated transients typically lack a plateau and this duration measure is therefore much prolonged by small changes in amplitude. There were no drug effects on the offset of the posttransient baseline.

After injury, field stimulation–induced transients were decreased as we have previously reported.[7] The effect of injury on sensitivity to blockers seen during field stimulation largely confirms findings during K^+ stimulation (fig. 5). Specifically, small axotomized L5 neurons showed decreased responses to N- and R-type blockers, whereas large L5 neurons showed decreased responses to N- and P/Q-type blockers. A significant increase in responsiveness to the dihydropyridine blockers nitrendipine and nisoldipine was seen in L4 neurons after SNL.

Discussion

Mammalian sensory neurons are equipped with a diversity of voltage-gated Ca^{2+} channel subtypes that regulate varied physiologic functions.[2] Exploration of their distinct roles was initiated by the observation of the selective inhibition of L-type current by dihydropyridines and by the discovery of natural snail and spider peptide toxins that discriminate between other high-voltage–activated Ca^{2+} currents. Our strategy in this study was to use the selective actions of various blockers, including the synthetic peptide analogs of invertebrate toxins, to identify the contributions of different channel subtypes to the intracellular Ca^{2+} signal that follows DRG neuron activation. Nonetheless, we recognize that there is imperfect selectivity of these agents. For example, nicardipine may block T-type currents,[35] and for this reason we also used nisoldipine and nitrendipine, which may also block a portion of the N-type current.[25] Selective block of T-type current is particularly problematic because all available agents have activity on secondary channel targets. We chose mibefradil because of its fairly selective profile[22] compared with amiloride and nickel, although it may also affect R-type[36] and L-type[32] currents at much higher concentrations than used here. Even the peptide blockers may have minor overlapping effects.[27]

Our findings with K^+ stimulation show that all high-voltage–activated I_{Ca} subtypes contribute to Ca^{2+} transients in sensory neurons activated this way, although the L- and N-type channels provide the dominant pathway, especially in large neurons. The substantial contribution of L-type channels to the K^+-triggered transient may be emphasized by the sustained depolarization generated by this type of neuronal activation, because L-type current minimally inactivates.[25] This is confirmed by our observation of a minimal sensitivity of field-evoked transients to dihydropyridine blockade of L-type channels, as also observed by others,[37,38] and a relatively greater percentile representation of transient sensitivity to other high-voltage–activated channel blockers. This pattern of relative contribution to the field-stimulated transient is similar to the pattern of specific channel subtype contributions to the total inward Ca^{2+} flux during membrane depolarization. Specifically, direct current measure by patch clamp technique shows that N- and P/Q-type predominate,[25,39,40] although there are subgroups of neurons that may have larger representation of L-type current.[11,34,41] Although our findings do not let us conclude that there is a simple linear relation between current flux and generation of the transient for each channel subtype, because of the complex modulation of the transient by intracellular processes,[42] the *pro rata* relation between current and transient broadly indicates a lack of specialization of the voltage-gated Ca^{2+} channel subtypes in initiating the cytoplasmic Ca^{2+} signal.

Our examination of injured neurons shows that axotomy selectively reduces the contribution of I_{Ca} subtypes to the generation of the Ca^{2+} transient on a cell size–specific basis. Specifically, using both high K^+ and field stimulation, axotomy of small neurons results in a diminished contribution to the transient by I_{Ca} through N- and R-type channels, whereas axotomy of large neurons decreases the component of the transient triggered by current through N- and P/Q-type channels. One study directly examining membrane Ca^{2+} flux has found a nonselective effect of axotomy on the various I_{Ca} subtypes,[41] but another has observed a particular loss of N-type current.[43] Our current observations also support a loss of the N-type contribution to the intracellular Ca^{2+} transient after axotomy, as well as loss of P/Q- and R-type components. N-type loss is most evident with sustained stimulation during K^+ application, whereas R-type is fully eliminated only in field stimulation that creates brief action potentials. There has been no previous report of axotomy-induced loss of R- or P/Q-type I_{Ca}. A different pattern is seen in the adjacent L4 neurons after SNL injury, in which the R-type contribution is decreased loss in small neurons, whereas the effect of L-type channel block depends on method of neuronal activation. The divergent responses comparing field and K^+ stimulation may indicate an injury effect on L4 neurons involving kinetics of channel activation or inactivation.

The mechanism by which injury causes Ca^{2+} channel contributions to the intracellular transient to diminish is unknown. The transcription of the genes coding for the channel subunits conducting L- and T-type currents are down-regulated after axotomy,[44] but transcription of

genes coding for N-, P/Q-, and R-type subunits is unchanged.[44,45] Therefore, regulation of transcription alone cannot explain our findings. Injury also modulates translation factors that regulate gene expression at a posttranscriptional level,[46] which could contribute to modulation of Ca^{2+} channel proteins, as has been noted for Na^{+} channels.[47] The observation of unchanged N-type channel protein in DRG neurons after axotomy[45] indicates that regulation of Ca^{2+} currents by intracellular signaling cascades and kinase activity may be an important cause of injury-induced phenotypic change.[48,49] Finally, sensory neuron injury is associated with slight but significant depolarization of the resting membrane potential,[50] which can alter the inactivation state of voltage-gated Ca^{2+} channels in a subtype-specific manner and alter the contribution of a particular subtype.

Decreased accumulation of cytoplasmic Ca^{2+} in peripheral neurons increases excitability and may contribute to generation neuropathic pain.[50–52] Ultimately, identification of the specific channel subtype or subtypes that are lost after injury may allow treatment that selectively enhances only the affected channels. Because the injury-associated changes are cell-size specific, such treatment may be designed to specifically alter neurons with nociceptive modality.

References

1. Thayer SA, Miller RJ: Regulation of the intracellular free calcium concentration in single rat dorsal root ganglion neurones *in vitro*. J Physiol 1990; 425:85–115
2. Ghosh A, Greenberg ME: Calcium signaling in neurons: Molecular mechanisms and cellular consequences. Science 1995; 268:239–47
3. Zucker RS, Regehr WG: Short-term synaptic plasticity. Annu Rev Physiol 2002; 64:355–405
4. Hogan QH, McCallum JB, Sarantopoulos C, Aason M, Mynlieff M, Kwok WM, Bosnjak ZJ: Painful neuropathy decreases membrane calcium current in mammalian primary afferent neurons. Pain 2000; 86:43–53
5. McCallum JB, Fuchs A, Poroli M, Hogan QH: Nerve injury decreases CaV2.2 conductance. Soc Neurosci Abstracts 2005; Program No. 35.12
6. Fuchs A, Lirk P, Stucky C, Abram SE, Hogan QH: Painful nerve injury decreases resting cytosolic calcium concentrations in sensory neurons of rats. ANESTHESIOLOGY 2005; 102:1217–25
7. Fuchs A, Rigaud M, Hogan Q: Painful nerve injury shortens the intracellular Ca^{2+} signal in axotomized sensory neurons of rats. ANESTHESIOLOGY 2007; 107: 106–16
8. Tsien RW, Lipscombe D, Madison D, Bley K, Fox A: Reflections on Ca(2+)-channel diversity, 1988-1994. Trends Neurosci 1995; 18:52–4
9. Varadi G, Strobeck M, Koch S, Caglioti L, Zucchi C, Palyi G: Molecular elements of ion permeation and selectivity within calcium channels. Crit Rev Biochem Mol Biol 1999; 34:181–214
10. Catterall WA: Structure and regulation of voltage-gated Ca2+ channels. Annu Rev Cell Dev Biol 2000; 16:521–55
11. Scroggs RS, Fox AP: Calcium current variation between acutely isolated adult rat dorsal root ganglion neurons of different size. J Physiol 1992; 445: 639–58
12. Miljanich GP, Ramachandran J: Antagonists of neuronal calcium channels: Structure, function, and therapeutic implications. Ann Rev Pharmacol Toxicol 1995; 35:707–34
13. Robitaille R, Garcia ML, Kaczorowski GJ, Charlton MP: Functional colocalization of calcium and calcium-gated potassium channels in control of transmitter release. Neuron 1993; 11:645–55
14. Sommer C, Schafers M: Painful mononeuropathy in C57BL/Wld mice with delayed wallerian degeneration: Differential effects of cytokine production and nerve regeneration on thermal and mechanical hypersensitivity. Brain Res 1998; 784:154–62
15. Stoll G, Jander S, Myers RR: Degeneration and regeneration of the peripheral nervous system: From Augustus Waller's observations to neuroinflammation. J Peripher Nerv Syst 2002; 7:13–27
16. Kim SH, Chung JM: An experimental model for peripheral neuropathy produced by segmental spinal nerve ligation in the rat. Pain 1992; 50:355–63
17. Hogan Q, Sapunar D, Modric-Jednacak K, McCallum JB: Detection of neuropathic pain in a rat model of peripheral nerve injury. ANESTHESIOLOGY 2004; 101:476–87
18. Grynkiewicz G, Poenie M, Tsien RY: A new generation of Ca2+ indicators with greatly improved fluorescence properties. J Biol Chem 1985; 260:3440–50
19. Werth JL, Thayer SA: Mitochondria buffer physiological calcium loads in cultured rat dorsal root ganglion neurons. J Neurosci 1994; 14:348–56
20. Mintz IM, Venema VJ, Swiderek KM, Lee TD, Bean BP, Adams ME: P-type calcium channels blocked by the spider toxin omega-Aga-IVA. Nature 1992; 355:827–9
21. Newcomb R, Szoke B, Palma A, Wang G, Chen X, Hopkins W, Cong R, Miller J, Urge L, Tarczy-Hornoch K, Loo JA, Dooley DJ, Nadasdi L, Tsien RW, Lemos J, Miljanich G: Selective peptide antagonist of the class E calcium channel from the venom of the tarantula Hysterocrates gigas. Biochemistry 1998; 37: 15353–62
22. McDonough SI, Bean BP: Mibefradil inhibition of T-type calcium channels in cerebellar Purkinje neurons. Mol Pharmacol 1998; 54:1080–7
23. Wang YX, Bezprozvannaya S, Bowersox SS, Nadasdi L, Miljanich G, Mezo G, Silva D, Tarczy-Hornoch K, Luther RR: Peripheral *versus* central potencies of N-type voltage-sensitive calcium channel blockers. Naunyn Schmiedebergs Arch Pharmacol 1998; 357:159–68
24. Scroggs RS, Fox AP: Distribution of dihydropyridine and omega-conotoxin-sensitive calcium currents in acutely isolated rat and frog sensory neuron somata: Diameter-dependent L channel expression in frog. J Neurosci 1991; 11:1334–46
25. Regan LJ, Sah DW, Bean BP: Ca2+ channels in rat central and peripheral neurons: High-threshold current resistant to dihydropyridine blockers and omega-conotoxin. Neuron 1991; 6:269–80
26. Hilaire C, Diochot S, Desmadryl G, Baldy-Moulinier M, Richard S, Valmier J: Opposite developmental regulation of P- and Q-type calcium currents during ontogenesis of large diameter mouse sensory neurons. Neuroscience 1996; 75: 1219–29
27. Burley JR, Dolphin AC: Overlapping selectivity of neurotoxin and dihydropyridine calcium channel blockers in cerebellar granule neurones. Neuropharmacology 2000; 39:1740–55
28. Holz GGT, Dunlap K, Kream RM: Characterization of the electrically evoked release of substance P from dorsal root ganglion neurons: Methods and dihydropyridine sensitivity. J Neurosci 1988; 8:463–71
29. Kruglikov I, Gryshchenko O, Shutov L, Kostyuk E, Kostyuk P, Voitenko N: Diabetes-induced abnormalities in ER calcium mobilization in primary and secondary nociceptive neurons. Pflugers Arch 2004; 448:395–401
30. Lee KH, Chung K, Chung JM, Coggeshall RE: Correlation of cell body size, axon size, and signal conduction velocity for individually labelled dorsal root ganglion cells in the cat. J Comp Neurol 1986; 243:335–46
31. Tsien RW, Lipscombe D, Madison DV, Bley KR, Fox AP: Multiple types of neuronal calcium channels and their selective modulation. Trends Neurosci 1988; 11:431–8
32. Viana F, Van den Bosch L, Missiaen L, Vandenberghe W, Droogmans G, Nilius B, Robberecht W: Mibefradil (Ro 40-5967) blocks multiple types of voltage-gated calcium channels in cultured rat spinal motoneurones. Cell Calcium 1997; 22:299–311
33. Eller P, Berjukov S, Wanner S, Huber I, Hering S, Knaus HG, Toth G, Kimball SD, Striessnig J: High affinity interaction of mibefradil with voltage-gated calcium and sodium channels. Br J Pharmacol 2000; 130:669–77
34. Cardenas CG, Del Mar LP, Scroggs RS: Variation in serotonergic inhibition of calcium channel currents in four types of rat sensory neurons differentiated by membrane properties. J Neurophysiol 1995; 74:1870–9
35. Richard S, Diochot S, Nargeot J, Baldy-Moulinier M, Valmier J: Inhibition of T-type calcium currents by dihydropyridines in mouse embryonic dorsal root ganglion neurons. Neurosci Lett 1991; 132:229–34
36. Randall AD, Tsien RW: Contrasting biophysical and pharmacological properties of T-type and R-type calcium channels. Neuropharmacology 1997; 36: 879–93
37. Piser TM, Lampe RA, Keith RA, Thayer SA: Omega-grammotoxin blocks action-potential-induced Ca2+ influx and whole-cell Ca2+ current in rat dorsal-root ganglion neurons. Pflugers Arch 1994; 426:214–20
38. Sipahimalani AS, Werth JL, Michelson RH, Dutta AK, Efange SM, Thayer SA: Lipophilic amino alcohols with calcium channel blocking activity. Biochem Pharmacol 1992; 44:2039–46
39. Mintz IM, Adams ME, Bean BP: P-type calcium channels in rat central and peripheral neurons. Neuron 1992; 9:85–95
40. Rusin KI, Moises HC: Mu-opioid receptor activation reduces multiple components of high-threshold calcium current in rat sensory neurons. J Neurosci 1995; 15:4315–27
41. Abdulla FA, Smith PA: Axotomy- and autotomy-induced changes in Ca2+ and K+ channel currents of rat dorsal root ganglion neurons. J Neurophysiol 2001; 85:644–58
42. Catterall WA: From ionic currents to molecular mechanisms: The structure and function of voltage-gated sodium channels. Neuron 2000; 26:13–25
43. Baccei ML, Kocsis JD: Voltage-gated calcium currents in axotomized adult rat cutaneous afferent neurons. J Neurophysiol 2000; 83:2227–38
44. Kim DS, Yoon CH, Lee SJ, Park SY, Yoo HJ, Cho HJ: Changes in voltage-

gated calcium channel alpha(1) gene expression in rat dorsal root ganglia following peripheral nerve injury. Brain Res Mol Brain Res 2001; 96:151–6

45. Luo ZD, Chaplan SR, Higuera ES, Sorkin LS, Stauderman KA, Williams ME, Yaksh TL: Upregulation of dorsal root ganglion (alpha)2(delta) calcium channel subunit and its correlation with allodynia in spinal nerve-injured rats. J Neurosci 2001; 21:1868–75

46. Xiao HS, Huang QH, Zhang FX, Bao L, Lu YJ, Guo C, Yang L, Huang WJ, Fu G, Xu SH, Cheng XP, Yan Q, Zhu ZD, Zhang X, Chen Z, Han ZG, Zhang X: Identification of gene expression profile of dorsal root ganglion in the rat peripheral axotomy model of neuropathic pain. Proc Natl Acad Sci U S A 2002; 99:8360–5

47. Pertin M, Ji RR, Berta T, Powell AJ, Karchewski L, Tate SN, Isom LL, Woolf CJ, Gilliard N, Spahn DR, Decosterd I: Upregulation of the voltage-gated sodium channel beta2 subunit in neuropathic pain models: Characterization of expression in injured and non-injured primary sensory neurons. J Neurosci 2005; 25:10970–80

48. Dolphin AC: Facilitation of Ca2+ current in excitable cells. Trends Neurosci 1996; 19:35–43

49. Ji RR, Shi TJ, Xu ZQ, Zhang Q, Sakagami H, Tsubochi H, Kondo H, Hokfelt T: Ca2+/calmodulin-dependent protein kinase type IV in dorsal root ganglion: Colocalization with peptides, axonal transport and effect of axotomy. Brain Res 1996; 721:167–73

50. Sapunar D, Ljubkovic M, Lirk P, McCallum JB, Hogan QH: Distinct membrane effects of spinal nerve ligation on injured and adjacent dorsal root ganglion neurons in rats. ANESTHESIOLOGY 2005; 103:360–76

51. Abdulla FA, Smith PA: Axotomy- and autotomy-induced changes in the excitability of rat dorsal root ganglion neurons. J Neurophysiol 2001; 85: 630–43

52. Luscher C, Lipp P, Luscher HR, Niggli E: Control of action potential propagation by intracellular Ca2+ in cultured rat dorsal root ganglion cells. J Physiol 1996; 490(pt 2):319–24